

## Temperature dependence of the direct band gap of $\text{In}_x\text{Ga}_{1-x}\text{As}$ ( $x=0.06$ and $0.15$ )

Z. Hang,\* D. Yan, and Fred H. Pollak\*

*Physics Department, Brooklyn College of the City University of New York, Brooklyn, New York 11210*

G. D. Pettit and J. M. Woodall

*IBM Thomas J. Watson Research Center, Yorktown Heights, New York 10598*

(Received 17 January 1991)

Photorefectance has been used to measure the direct band gap of  $\text{In}_x\text{Ga}_{1-x}\text{As}$  ( $x=0.06$  and  $0.15$ ) over a wide temperature range from 18 to 873 K. We have evaluated the parameters that describe the temperature dependence of the band gap and broadening function.

The ability to perform optical experiments on semiconductors over a wide temperature range, including elevated temperatures, has many fundamental<sup>1-6</sup> as well as applied ramifications.<sup>7-10</sup> The temperature dependence of the energy and broadening of interband electronic transitions can yield important information about electron-phonon interactions, excitonic effects, etc.<sup>1-6</sup> An increase in temperature leads to a redshift of band gaps and an increase in the linewidth. The temperature variation of energy gaps can be described by equations involving three parameters such as the Varshni expression<sup>1</sup> or the more recently proposed term containing the Bose-Einstein occupation factor for phonons.<sup>1-6</sup> A similar Bose-Einstein equation also has been used to fit the temperature dependence of the broadening function.<sup>5,6</sup> Experimental values of these parameters can be used to test theories.<sup>4-6</sup> From an applied point of view, the ability to measure the band gap at the elevated temperatures ( $\sim 600^\circ\text{C}$ ) corresponding to the growth conditions of molecular-beam epitaxy (MBE), metal-organic-chemical vapor deposition (MOCVD), or gas phase molecular-beam epitaxy (GPMBE) opens up many new possibilities. For example, (a) the temperature of a substrate material (GaAs or InP) or (b) the alloy composition of  $\text{Ga}_{1-x}\text{Al}_x\text{As}$  or  $\text{In}_x\text{Ga}_{1-x}\text{As}$  could be monitored *in situ* during actual growth procedures.<sup>7-10</sup>

The semiconductor  $\text{In}_x\text{Ga}_{1-x}\text{As}$  is an important material for both fundamental research and device applications. It is a model material for high speed devices<sup>12</sup> such as high electron mobility transistors and field-effect transistors because of its small electron effective mass and high electron mobility. It is also used to fabricate quantum confinement heterostructure lasers,<sup>13</sup> in which the desired optical properties can be achieved by controlling the indium composition and the thickness of layers in the quantum wells.

In this paper we report photorefectance<sup>14</sup> (PR) measurements of the direct gap ( $E_0$ ) of undoped, strain-relieved  $\text{In}_x\text{Ga}_{1-x}\text{As}/\text{GaAs}$  ( $x=0.06$  and  $0.15$ ) from 18 K to  $600^\circ\text{C}$  in the photon energy range from 0.9 to 1.5 eV. Photorefectance is a contactless form of electromodulation.<sup>14</sup> We have analyzed the temperature dependence of  $E_0$  by both Varshni<sup>11</sup> and Bose-Einstein expres-

sions.<sup>1-6</sup> Because of the relatively low indium composition of our samples these parameters are similar to those of GaAs.<sup>1</sup> By taking into account the component of the energy gap shift due to the thermal expansion coefficient, we have obtained revised parameters which are directly related to the electron-phonon interaction.<sup>8</sup> The temperature variation of the broadening parameter  $\Gamma$  has been studied in terms of a Bose-Einstein expression. We find that while both acoustic and optical phonons participate in the energy shift only the electron-optical-phonon interaction is responsible for the changes in linewidth. Using PR,<sup>7-10</sup> it has been possible to observe  $E_0$  to temperatures which are a factor of 2 higher in relation to recently reported spectral ellipsometry results on GaAs (Ref. 1) and InP.<sup>2</sup> This is probably due to the fact that the electromodulation spectrum<sup>15</sup> is not only proportional to the third derivative of the dielectric function but is inversely proportional to the reduced interband mass ( $\mu$ ) while the ellipsometry signal is proportional to  $\mu^{3/2}$ .

The measurements were performed on two epitaxial layers of (100)  $\text{In}_x\text{Ga}_{1-x}\text{As}$  (undoped) of thickness 1.5 and  $1.0\ \mu\text{m}$  for  $x=0.06$  and  $0.15$ , respectively, grown on  $0.5\ \mu\text{m}$  of GaAs buffers (undoped) on GaAs (undoped) substrates. The growth procedure was MBE. The indium compositions of 0.06 and 0.15 were determined from  $E_0$  at 300 K using the relation<sup>16</sup>  $E_0(\text{In}_x\text{Ga}_{1-x}\text{As}) = E_0(\text{GaAs}) - 1.53x + 0.45x^2$ . These values were close to those estimated from the growth conditions. For these thicknesses of the epitaxial layers the lattice-mismatched strain should be completely relaxed.<sup>17</sup> This relaxation was confirmed by x-ray measurements on both samples.

The PR apparatus<sup>18</sup> and heater arrangement<sup>7,8</sup> were similar to those already reported in the literature. The temperature was measured by an iron-constant thermocouple in contact with the sample surface. For measurements up to about  $200^\circ\text{C}$  the pump beam was the  $6328\text{-\AA}$  line of a 3-mW He-Ne laser chopped at 851 Hz. Above this temperature 300 mW of the  $6471\text{-\AA}$  line of a Kr-ion laser was employed.

Displayed by the dotted lines in the top and bottom of Fig. 1 are the PR spectra of the  $\text{In}_{0.06}\text{Ga}_{0.94}\text{As}$  and  $\text{In}_{0.15}\text{Ga}_{0.85}\text{As}$  samples, respectively, at  $25^\circ\text{C}$ ,  $325^\circ\text{C}$ , and  $600^\circ\text{C}$ . The solid lines are least-squares fits to the third-

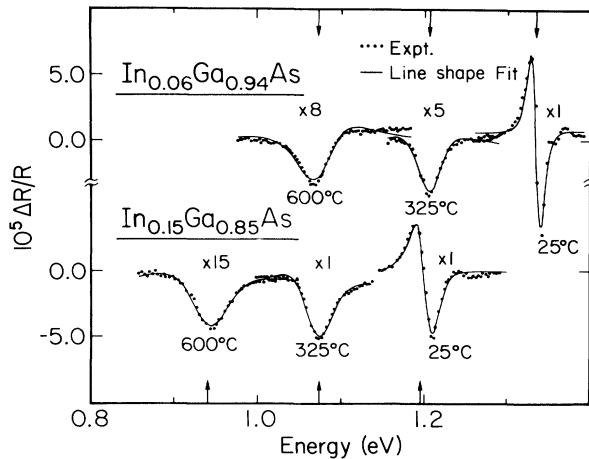


FIG. 1. Photoreflectance spectra (dotted lines) of the direct gap of  $\text{In}_x\text{Ga}_{1-x}\text{As}$  ( $x=0.06$  and  $0.15$ ) at  $25^\circ\text{C}$ ,  $325^\circ\text{C}$ , and  $600^\circ\text{C}$ . The solid line is a least-squares fit to a third-derivative functional form line shape.

derivative functional form (TDF) for a three-dimensional critical point.<sup>15</sup> The obtained values of  $E_0$  are designated by arrows in the figure. The fit also yielded the broadening parameter. Due to piezoelectric effects<sup>19</sup> there may sometimes be an additional first-derivative Lorentzian component to the TDF fit.<sup>20</sup> However, such terms are generally small unless the material contains a high concentration of defects.<sup>20</sup> The quality of the TDF fit to our data certainly indicates that such first-derivative terms are negligible.

We have observed that at  $25^\circ\text{C}$  and below, the spectra exhibited Franz-Keldysh oscillations (FKO's) above the band gap.<sup>15,21</sup> For example, one FKO can be detected in the  $25^\circ\text{C}$  spectra of both samples in Fig. 1. The small number of FKO's indicates that we are close to the low-field regime and hence the TDF fit is applicable.<sup>15,21</sup> At lower temperatures more FKO's become evident because of the decrease in the linewidth. In this regime, the energy gap and broadening parameter were obtained from the three point method.<sup>15</sup> The origin of these FKO's will be the subject of a planned future paper.<sup>22</sup>

We also attempted to fit the  $25^\circ\text{C}$  spectra for both samples with a first-derivative Gaussian functional form (FDGF).<sup>23</sup> The TDF, which is appropriate for unbound band-to-band transitions,<sup>17</sup> yielded a better fit than the FDGF, a line shape which represents transitions associated with bound states such as excitons.<sup>23</sup> This FDGF has a different physical origin in relation to the possible first-derivative Lorentzian term discussed above. The lack of an excitonic contribution is not unreasonable since for these samples the linewidth at  $25^\circ\text{C}$  and above ( $\geq 15$  meV) is greater than the exciton binding energy.<sup>24</sup> It is interesting to note that for bulk InP excitonic contributions in the PR spectra were observed up to about  $300^\circ\text{C}$ .<sup>8</sup>

Plotted in Fig. 2 are the temperature variations of  $E_0$

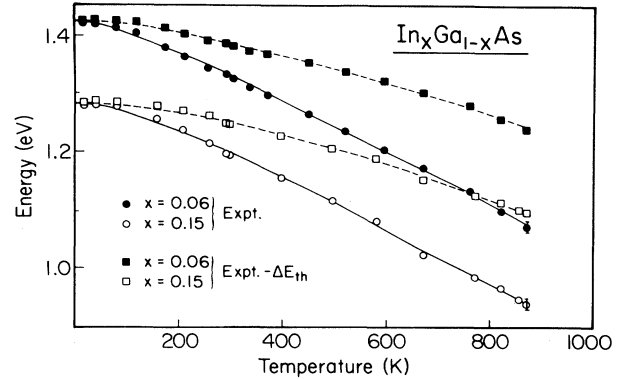


FIG. 2. The experimental temperature dependence of  $E_0$  of  $\text{In}_x\text{Ga}_{1-x}\text{As}$  for  $x=0.06$  (closed circles) and  $0.15$  (open circles). The closed and open squares are the data minus the thermal expansion contribution,  $\Delta E_{\text{th}}$ , for the  $x=0.06$  and  $0.15$  samples, respectively. The solid and dashed lines are least-squares fits to Eqs. (1) and (5), respectively.

for the  $x=0.06$  (closed circles) and  $0.15$  (open circles) samples. Representative error bars are shown. The solid lines are least-squares fits to the Varshni semiempirical relationship:<sup>11</sup>

$$E_0(T) = E_0(0) - \alpha T^2 / (\beta + T) . \quad (1)$$

The obtained values of  $E_0(0)$ ,  $\alpha$  and  $\beta$  for both samples are listed in Table I. For comparison, we have also listed in Table I the values of these quantities for GaAs obtained by previous investigators.<sup>1,7</sup> The values  $\alpha$  and  $\beta$  for the  $\text{In}_x\text{Ga}_{1-x}\text{As}$  samples are found to be similar to those of GaAs because of the low In concentration of the layers.

The data have also been fit to the Bose-Einstein expression proposed by Lautenschlager *et al.*:<sup>1,5</sup>

$$E_0(T) = E_B - a_B \{ 1 + 2 / [\exp(\Theta_B / T) - 1] \} , \quad (2)$$

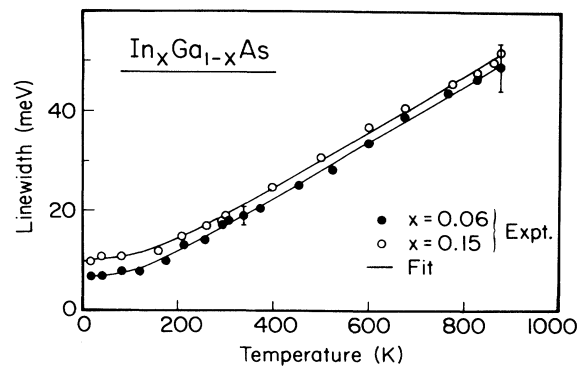


FIG. 3. The temperature variation of the broadening parameter for the  $x=0.06$  (closed circles) and  $0.15$  (open circles) samples. The solid lines are least-squares fits to Eq. (3).

TABLE I. Values of the parameters which describe the temperature dependence of the direct energy band gaps of  $\text{In}_x\text{Ga}_{1-x}\text{As}$  and GaAs.

Material	$E_0(0)$ (eV)	$\alpha$ ( $10^{-4}$ eV/K)	$\beta$ (K)	$E_B$ (eV)	$a_B$ (meV)	$\Theta_B$ (K)
$\text{In}_{0.06}\text{Ga}_{0.94}\text{As}$	$1.420 \pm 0.005$	$4.8 \pm 0.4$	$200 \pm 50$	$1.466 \pm 0.014$	$44 \pm 9$	$203 \pm 45$
$\text{In}_{0.15}\text{Ga}_{0.85}\text{As}$	$1.285 \pm 0.005$	$5.0 \pm 0.4$	$231 \pm 40$	$1.339 \pm 0.015$	$53 \pm 10$	$238 \pm 50$
GaAs	$1.512 \pm 0.005^a$ $1.517 \pm 0.008^b$	$5.1 \pm 0.5^a$ $5.5 \pm 1.3^b$	$190 \pm 82^a$ $225 \pm 174^b$	$1.571 \pm 0.023^b$	$57 \pm 29^b$	$240 \pm 102^b$

<sup>a</sup>From Ref. 7.

<sup>b</sup>From Ref. 1.

where  $a_B$  represents the strength of the electron-phonon interaction and  $\Theta_B$  corresponds to the average phonon temperature. Our numbers for  $E_B$ ,  $a_B$ , and  $\Theta_B$  are given in Table I; also listed are the corresponding values for GaAs.<sup>1</sup>

The temperature dependence of  $\Gamma$  for both  $\text{In}_{0.06}\text{Ga}_{0.94}\text{As}$  (closed circles) and  $\text{In}_{0.15}\text{Ga}_{0.85}\text{As}$  (open circles) samples are displayed in Fig. 3. Representative error bars are shown. The solid line is a least-squares fit to the equation<sup>1,5,6</sup>

$$\Gamma(T) = \Gamma_0 + \Gamma_1 / [\exp(\Theta/T) - 1] \quad (3)$$

The values of  $\Gamma_0$ ,  $\Gamma_1$ , and  $\Theta$  corresponding to the broadening parameter of  $E_0$  are listed in Table II. Also given in Table II are the corresponding numbers for GaAs.<sup>1</sup> The first term of Eq. (3) corresponds to broadening mechanisms due to intrinsic lifetime, electron-electron interaction, impurity, dislocation, and alloy scattering effects. The obtained value of  $\Gamma_0$  for the  $x=0.15$  sample is larger than that for the  $x=0.06$  material and both are significantly greater than expected from alloy scattering ( $\sim 2$  meV).<sup>25</sup> These results are probably related to the relatively high concentration of misfit locations associated with the strain relief. For example, the linear density of dislocations for the former sample is about a factor 2 greater in relation to the latter material.<sup>26</sup>

The second term of Eq. (3) corresponds to the lifetime broadening due to the electron-optical-phonon interaction. The quantity  $\Gamma_1$  represents the strength of the electron-optical-phonon coupling while  $\Theta$  is the optical-phonon temperature. For comparison we have measured the ‘‘GaAs-like’’ ( $\Theta_{\text{LO1}}$ ) and ‘‘InAs-like’’ ( $\Theta_{\text{LO2}}$ ) longitudinal-optical- (LO) phonon temperatures for the two samples using Raman scattering.<sup>27</sup> These values also

are presented in Table II. As can be seen our numbers for  $\Theta$  are quite close to  $\Theta_{\text{LO1}}$  and  $\Theta_{\text{LO2}}$  for both samples.

Due to the low In composition of our samples  $\Gamma_1$  and  $\Theta$  for InGaAs should be similar to those of GaAs.<sup>1</sup> However, because of the larger error margins of the data from Ref. 1 comparison is hard to make although there are no inconsistencies. Our values for these parameters are more accurate since our maximum temperature was about a factor of 3 greater than that of Ref. 1 for the determination of the temperature variation of  $\Gamma$ .

The temperature shift of  $E_0$  contains contributions from both thermal expansion and electron-phonon coupling effects.<sup>8,28</sup> Therefore, in order to obtain parameters directly related to the latter influence, it is necessary to eliminate the contribution of the former. For example, the quantities  $\alpha$  and  $\beta$  of Eq. (1) and  $a_B$  and  $\Theta_B$  of Eq. (2) include the influence of the lattice dilation. The energy shift  $\Delta E_{\text{th}}$  due to the thermal expansion can be written as

$$\Delta E_{\text{th}} = -3\alpha\alpha_{\text{th}}T, \quad (4)$$

where  $\alpha$  is the hydrostatic deformation potential and  $\alpha_{\text{th}}$  is the linear expansion coefficient. For our samples we have obtained the values of  $\alpha$  and  $\alpha_{\text{th}}$  listed in Table III by a linear interpolation between the corresponding coefficients of GaAs and InAs.<sup>29</sup> For the latter quantity we have used the average thermal expansion coefficient of the end point materials since the temperature dependence of  $\alpha_{\text{th}}$  (InAs) is not known. Equations (1) and (2) can be rewritten as

$$E_0(T) - \Delta E_{\text{th}} = E_0(0) - \alpha'T^2/(\beta' + T), \quad (5)$$

$$E_0(T) - \Delta E_{\text{th}} = E'_B - a'_B \{1 + 2/[\exp(\Theta'_B/T) - 1]\}. \quad (6)$$

The solid ( $x=0.06$ ) and open ( $x=0.15$ ) squares in Fig. 1 represent data which result from subtracting  $\Delta E_{\text{th}}$

TABLE II. Parameters involved in the temperature dependence of the broadening parameter of  $E_0$  of  $\text{In}_x\text{Ga}_{1-x}\text{As}$  ( $x=0.06$  and  $0.15$ ) using the fit  $\Gamma(T) = \Gamma_0 + \Gamma_1 / [\exp(\Theta/T) - 1]$ .

Materials	$\Gamma_0$ (meV)	$\Gamma_1$ (meV)	$\Theta$ (K)	$\Theta_{\text{LO1}}$ (K)	$\Theta_{\text{LO2}}$ (K)
6%	$7.5 \pm 0.5$	$23 \pm 6$	$370 \pm 122$	$410^a$	$376^a$
15%	$10.5 \pm 0.5$	$23 \pm 6$	$380 \pm 120$	$406^a$	$375^a$

<sup>a</sup>Longitudinal-optical-phonon temperatures for the ‘‘GaAs-like’’ ( $\Theta_{\text{LO1}}$ ) and ‘‘InAs-like’’ ( $\Theta_{\text{LO2}}$ ) modes of  $\text{In}_{1-x}\text{Ga}_x\text{As}$  obtained from Raman measurements.

TABLE III. Values of the parameters which describe the temperature dependence of the direct energy gaps of  $\text{In}_x\text{Ga}_{1-x}\text{As}$  taking into account the effects of thermal expansion.

Materials	$\alpha_{\text{th}}$ ( $10^{-6}/\text{K}$ )	$\alpha$ (eV)	$\alpha'$ ( $10^{-4}$ eV/K)	$\beta'$ (K)	$E'_B$ (eV)	$a'_B$ (meV)	$\Theta'_B$ (K)	$\frac{3}{8}\Theta_D$ (K)
6%	6.69 <sup>a</sup>	-9.54 <sup>a</sup>	2.5±0.4	140±40	1.453±0.012	33±7	280±45	127 <sup>a</sup>
15%	6.48 <sup>a</sup>	-9.24 <sup>a</sup>	2.6±0.4	150±40	1.323±0.013	39±8	300±50	124 <sup>a</sup>

<sup>a</sup>The parameters of  $\alpha_{\text{th}}$ ,  $\alpha$ , and  $\Theta_D$  were estimated by using a linear interpolation between the values of GaAs and InAs as listed in Ref. 29.

[Eq. (4)] from the experimental values of  $E_0(T)$ . The dashed lines are least-squares fits to Eq. (5). These data have also been fit to Eq. (6). The obtained values of  $\alpha'$ ,  $\beta'$ ,  $E'_B$ ,  $a'_B$ , and  $\Theta'_B$  are listed in Table III.

From Tables II and III, it can be seen that the values of  $\Theta'_B$  are less than  $\Theta$ . Since both electron-optical- and electron-acoustic-phonon interactions contribute to the energy shift of the band gap,<sup>1,2,5,6</sup> this leads to a low average phonon temperature  $\Theta'_B$ . Since  $\Theta$  for both samples is quite similar to the LO-phonon temperatures ( $\Theta_{\text{LO1}}$  and  $\Theta_{\text{LO2}}$ ) the temperature variation of  $\Gamma$  is due mainly to the interaction of the electron with optical phonons. These observations are in agreement with existing theory.<sup>4,6</sup>

Manoogian and Woolley<sup>28</sup> have suggested that after the thermal expansion term is removed the parameter  $\beta'$  of Eq. (5) is directly proportional to the Debye temperature  $\Theta_D$  by the relation  $\beta' = \frac{3}{8}\Theta_D$ . Also listed in Table II are  $\Theta_D$  for the two In compositions estimated by linear interpolation between the end point binary materials.<sup>19</sup> As can be seen, there is good agreement between  $\beta'$  and  $\frac{3}{8}\Theta_D$ .

The parameter  $\alpha'$  of Eq. (5) can be related to  $a'_B$  and  $\Theta'_B$  of Eq. (6) by taking the high-temperature limit of both expressions. This yields  $\alpha' = 2a'_B/\Theta'_B$ . Table III

shows that this relation is indeed satisfied.

It can be seen from Fig. 1 that it is important to take into account the effect of the lattice dilation when evaluating the electron-phonon parameter related to the energy gap redshift. At 600°C the thermal expansion term corresponds to about 45% of the total variation for both samples.

In conclusion, we have measured the temperature dependence of the direct band gap and its broadening parameter for  $\text{In}_x\text{Ga}_{1-x}\text{As}$  ( $x=0.06$  and  $0.15$ ) in the temperature range 18 K to 600°C. We have analyzed  $E_0(T)$  in terms of both Varshni and Bose-Einstein expressions while the temperature variation of  $\Gamma(T)$  has been fitted to a Bose-Einstein equation. While both optical and acoustic phonons contribute to the redshift of  $E_0$ , only optical phonons participate in the temperature variation of the broadening function.

The authors Z.H., D.Y., and F.H.P. acknowledge the support of the IBM Shared University Research (SUR) program, NSF grant No. ECS-8913321, the McDonnell-Douglas Electronic Systems Company, and the New York State Science and Technology Foundation through its Centers for Advance Technology Program.

\*Also at Graduate School and University Center, City University of New York, New York, NY 10036.

<sup>1</sup>See, for example, P. Lautenschlager, M. Garriga, S. Logothetidis, and M. Cardona, Phys. Rev. B **35**, 9174 (1987), and references therein.

<sup>2</sup>See, for example, P. Lautenschlager, M. Garriga, and M. Cardona, Phys. Rev. B **36**, 4813 (1987), and references therein.

<sup>3</sup>P. Lautenschlager, P. B. Allen, and M. Cardona, Phys. Rev. B **33**, 5501 (1986).

<sup>4</sup>P. B. Allen and M. Cardona, Phys. Rev. B **23**, 1495 (1981).

<sup>5</sup>P. Lautenschlager, M. Garriga, L. Vina, and M. Cardona, Phys. Rev. B **36**, 4821 (1987).

<sup>6</sup>S. Gopalan, P. Lautenschlager, and M. Cardona, Phys. Rev. B **35**, 5577 (1987).

<sup>7</sup>See, for example, H. Shen, S. H. Pan, Z. Hang, J. Leng, F. H. Pollak, J. M. Woodall, and R. N. Sacks, Appl. Phys. Lett. **53**, 1080 (1988).

<sup>8</sup>Z. Hang, H. Shen, and F. H. Pollak, Solid State Commun. **73**, 15 (1990).

<sup>9</sup>Z. Hang, H. Shen, and F. H. Pollak, Proc. Soc. Photo-Opt. Instrum. Eng. **1285**, 14 (1990).

<sup>10</sup>F. H. Pollak, Proc. Soc. Photo-Opt. Instrum. Eng. **1361**, 109 (1991).

<sup>11</sup>Y. P. Varshni, Physica (Utrecht) **34**, 149 (1967).

<sup>12</sup>H. Morkoç and H. Unlu, in *Semiconductors and Semimetals*, edited by R. Dingle (Academic, New York, 1987), Vol. 24, p. 135.

<sup>13</sup>W. T. Tsang, in *Semiconductors and Semimetals*, edited by R. Dingle (Academic, New York, 1987), Vol. 24, p. 397.

<sup>14</sup>See, for example, F. H. Pollak and O. J. Glembocki, Proc. Soc. Photo-Opt. Instrum. Eng. **946**, 2 (1988).

<sup>15</sup>D. E. Aspnes, in *Handbook on Semiconductors*, edited by T. S. Moss (North-Holland, New York, 1980), Vol. 2, p. 109.

<sup>16</sup>S. Adachi, J. Appl. Phys. **58**, R1 (1985).

<sup>17</sup>See, for example, J. W. Mayer and S. S. Lau, *Electronic Materials Science For Integrated Circuits in Si and GaAs* (Macmillan, New York, 1990), p. 425.

<sup>18</sup>H. Shen, P. Parayanthal, Y. F. Liu, and F. H. Pollak, Rev. Sci.

- Instrum. **58**, 1429 (1987).
- <sup>19</sup>D. S. Kyser and V. Rehn, *Solid State Commun.* **8**, 1937 (1970).
- <sup>20</sup>P. M. Raccach, J. W. Garland, Z. Zhang, V. Lee, D. Z. Xue, L. L. Abels, S. Ugur, and W. Wilensky, *Phys. Rev. Lett.* **53**, 1958 (1984).
- <sup>21</sup>H. Shen and F. H. Pollak, *Phys. Rev. B* **42**, 7097 (1990).
- <sup>22</sup>Z. Hang, H. Shen, F. H. Pollak, G. D. Pettit, and J. M. Woodall (unpublished).
- <sup>23</sup>O. J. Glembocki and B. V. Shanabrook, *Superlatt. Microstruct.* **5**, 603 (1989).
- <sup>24</sup>Because both samples have low In concentrations, the exciton binding energy should be close to that of GaAs ( $\sim 5$  meV).
- The parameter  $\Gamma$  for both samples at room temperature is about 15 meV.
- <sup>25</sup>J. Singh and K. K. Bajaj, *Appl. Phys. Lett.* **48**, 1077 (1986).
- <sup>26</sup>J. M. Woodall, G. D. Pettit, T. N. Jackson, and C. Lanza, *Phys. Rev. Lett.* **51**, 1783 (1983).
- <sup>27</sup>F. H. Pollak and R. Tsu, *Proc. Soc. Photo-Opt. Instrum. Eng.* **452**, 26 (1984).
- <sup>28</sup>A. Manoogian and J. C. Woolley, *Can. J. Phys.* **62**, 285 (1984).
- <sup>29</sup>*Numerical Data and Functional Relationships in Science and Technology*, edited by O. Madelung, M. Schulz, and H. Weiss, Landolt-Börnstein, New Series, Group III, Vol. 17a (Springer, New York, 1982); *ibid.*, Vol. 22a.